Supporting Information to Comparison of 3D-cDFT and GCMC Simulations for Fluid-Structure Analysis in Amorphous Carbon Nanoporous Materials

Lucas J. dos Santos,[1] Elvis do A. Soares,[1] Amaro G. Barreto Jr.,[1] and Frederico W. Tavares[1,2,*]

[1] *Engenharia de Processos Químicos e Bioquímicos (EPQB), Escola de Química, Universidade Federal do Rio de Janeiro, 21941-909, Rio de Janeiro, RJ, Brazil*

[2] *Programa de Engenharia Química, COPPE, Universidade Federal do Rio de Janeiro, 21941-909, Rio de Janeiro, RJ, Brazil*

I. METHANE FLUID PARAMETERS

In this work, we used the JZG EoS to represent the thermodynamics of LJ fluids. For methane molecule can be approximated by a LJ particle as reported by the TraPPE force-field[S1], with the following parameters ($\sigma_{CH_4} = 3.73$ Å and $\epsilon_{CH_4}/k_B = 148.0$ K. The PC-SAFT [S2] also represents the methane molecule by a LJ particle with appropriate parameters ($m_{CH_4} = 1.0000$, $\sigma_{CH_4} = 3.7039$ Å, $\epsilon_{CH_4}/k_B = 150.03$ K). However, the dispersive contribution was calculated using a 2-order Baker-Henderson perturbation theory.

Figure S1 presents the Vapor-Liquid equibrium diagram and the vapor pressure of CH_4 calculated from the JZG EoS in comparison with the experimental data. The dashed and solid lines represent the JZG EoS calculated with the PC-SAFT and TraPPE parameters, respectively.

II. THE FUNDAMENTAL MEASURE THEORY

The functional F_{hs} represents the excess Helmholtz free-energy functional due to hard-sphere exclusion volume, which have been described by the modified fundamental measure theory (FMT)[S3]. In this work, we apply the White-Bear functional [S4, S5] for the hard-sphere Helmholtz free-energy contribution as

$$\beta F_{\text{hs}}[\rho(\boldsymbol{r})] = \int_{\mathcal{V}} \mathrm{d}\boldsymbol{r}\, \Phi_{\text{FMT}}(\{n_\alpha(\boldsymbol{r})\}), \tag{S1}$$

where the reduced free energy density of a mixture of hard-spheres, Φ_{FMT}, is a function of the set of weighted densities, $n_\alpha(\boldsymbol{r})$. Here, the free energy density $\Phi_{\text{FMT}}(\{n_\alpha(\boldsymbol{r})\})$ is based on the

* tavares@eq.ufrj.br

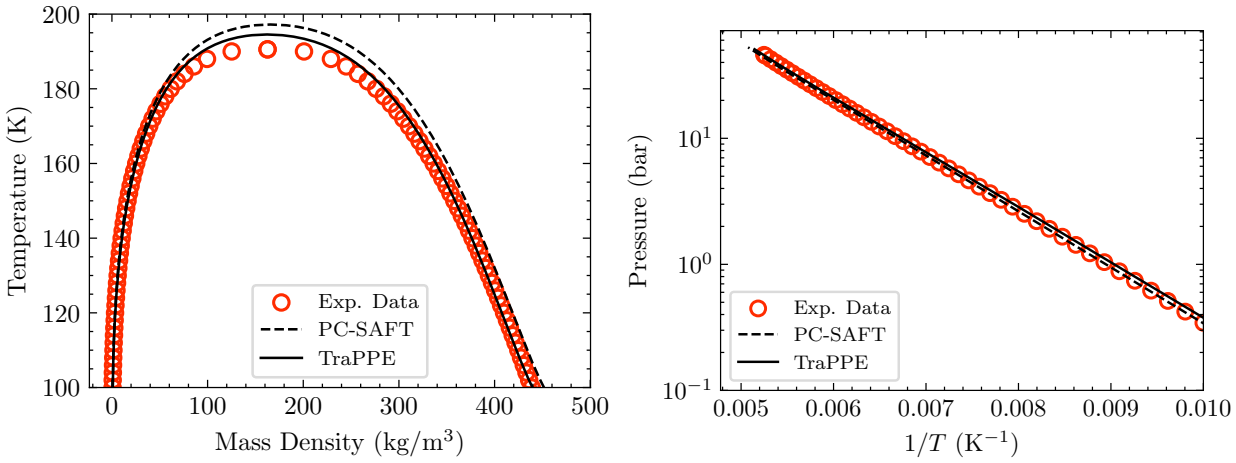

(a) CH_4 VLE Diagram

(b) CH_4 Vapor Pressure

FIG. S1. (a) Vapor-Liquid Equilibria (VLE) diagram of methane fluid. (b) Vapor pressure of methane fluid. Open symbols: Experimental Data. Lines: JZG EoS with PC-SAFT parameters (*dashed line*) and TraPPE parameters (*solid line*).

antisymmetrized version of the functional from Rosenfeld *et al.* [S6] given by

$$\Phi_{\mathrm{FMT}}(\{n_\alpha(\boldsymbol{r})\}) = \phi_1(n_3)n_0 + \phi_2(n_3)(n_1n_2 - \boldsymbol{n}_{v1}\cdot\boldsymbol{n}_{v2}) + \phi_3(n_3)n_2^3(1 - \boldsymbol{n}_{v2}\cdot\boldsymbol{n}_{v2}/n_2^2)^3, \tag{S2}$$

where the first two terms of the binomial expansion of $(1 - \boldsymbol{n}_{v2}\cdot\boldsymbol{n}_{v2}/n_2^2)^3$ recover the usual White Bear functional. As reported by Kessler *et al.* [S7] the resulting antisymmetrized functional yields accurate results for hard spheres in narrow cylindrical while retaining the full three-dimensional properties and the bulk behavior of the original White Bear functional.

The White-Bear mark I functions are defined as

$$\phi_1(n_3) = -\ln(1 - n_3), \tag{S3}$$

$$\phi_2(n_3) = \frac{1}{1 - n_3}, \tag{S4}$$

$$\phi_3(n_3) = \frac{2n_3 + 2(1 - n_3)^2\ln(1 - n_3)}{72\pi n_3^2(1 - n_3)^2}, \tag{S5}$$

with the weigthed densities defined as

$$n_\alpha(\boldsymbol{r}) \equiv \int_{\mathcal{V}} \mathrm{d}\boldsymbol{r}'\,\rho(\boldsymbol{r}')\omega^{(\alpha)}(\boldsymbol{r} - \boldsymbol{r}'), \tag{S6}$$

whose the linearly independent weights are defined as

$$\omega^{(3)}(\boldsymbol{r}) = \Theta(d/2 - |\boldsymbol{r}|), \tag{S7}$$

$$\omega^{(2)}(\boldsymbol{r}) = |\boldsymbol{\nabla}\Theta(d/2 - |\boldsymbol{r}|)| = \delta(d/2 - |\boldsymbol{r}|), \tag{S8}$$

$$\boldsymbol{\omega}^{(v2)}(\boldsymbol{r}) = \boldsymbol{\nabla}\Theta(d/2 - |\boldsymbol{r}|) = \frac{\boldsymbol{r}}{r}\delta(d/2 - |\boldsymbol{r}|), \tag{S9}$$

and the dependent weights given by $\omega^{(0)}(\boldsymbol{r}) = \omega^{(2)}(\boldsymbol{r})/\pi d^2$, $\omega^{(1)}(\boldsymbol{r}) = \omega^{(2)}(\boldsymbol{r})/2\pi d$, and $\boldsymbol{\omega}^{(v1)}(\boldsymbol{r}) = \boldsymbol{\omega}^{(v2)}(\boldsymbol{r})/2\pi d$. Here, $\Theta(r)$ is the Heaviside step function, $\delta(r)$ is the Dirac delta function, and d is the hard-sphere diameter. We can note that

$$\int_{\mathcal{V}} \omega^{(3)}(\boldsymbol{r})\,\mathrm{d}\boldsymbol{r} = 4\pi \int_0^\infty \Theta(d/2-|\boldsymbol{r}|)r^2\,\mathrm{d}r = \frac{\pi}{6}d^3, \tag{S10}$$

$$\int_{\mathcal{V}} \omega^{(2)}(\boldsymbol{r})\,\mathrm{d}\boldsymbol{r} = 4\pi \int \delta(d/2-|\boldsymbol{r}|)r^2\,\mathrm{d}r = \pi d^2, \tag{S11}$$

$$\int_{\mathcal{V}} \omega^{(v2)}(\boldsymbol{r})\,\mathrm{d}\boldsymbol{r} = 4\pi \int \frac{\boldsymbol{r}}{r}\delta(d/2-|\boldsymbol{r}|)r^2\,\mathrm{d}r = 0. \tag{S12}$$

The analytical Fourier transforms of these linearly independent weight functions are given in the form

$$\begin{aligned}\widetilde{\omega}^{(3)}(\boldsymbol{k}) &= \int \Theta(d/2-|\boldsymbol{r}|)e^{-i\boldsymbol{k}\cdot\boldsymbol{r}}\,\mathrm{d}^3r = 4\pi\int_0^\infty \mathrm{d}r\,\Theta(d/2-r)r^2\frac{\sin(kr)}{kr}\\ &= \frac{\pi d^2}{k}\left[\frac{\sin(kd/2)}{(kd/2)^2}-\frac{\cos(kd/2)}{kd/2}\right] = \frac{\pi d^2}{k}j_1(kd/2) = \frac{\pi d^3}{6}[j_0(kd/2)+j_2(kd/2)],\end{aligned} \tag{S13}$$

where we made use of the recurrence formula for the spherical Bessel functions, $j_{n-1}(x)+j_{n+1}(x) = \frac{2n+1}{x}j_n(x)$, and

$$\begin{aligned}\widetilde{\omega}^{(2)}(\boldsymbol{k}) &= \int \delta(d/2-|\boldsymbol{r}|)e^{-i\boldsymbol{k}\cdot\boldsymbol{r}}\,\mathrm{d}^3r = 4\pi\int_0^\infty \mathrm{d}r\,\delta(d/2-r)r^2\frac{\sin(kr)}{kr}\\ &= \pi d^2\frac{\sin(kd/2)}{kd/2} = \pi d^2 j_0(kd/2)\end{aligned} \tag{S14}$$

and

$$\widetilde{\boldsymbol{\omega}}^{(v2)}(\boldsymbol{k}) = -\frac{1}{id/2}\frac{\mathrm{d}}{\mathrm{d}\boldsymbol{k}}\left[\tilde{\omega}^{(2)}(\boldsymbol{k})\right] = -i\boldsymbol{k}\tilde{\omega}^{(3)}(\boldsymbol{k}) \tag{S15}$$

The chemical potential is obtained by the bulk composition as

$$\beta\mu^{\mathrm{hs}} = \frac{\partial\Phi^{(b)}_{\mathrm{FMT}}}{\partial\rho^{(b)}}. \tag{S16}$$

III. THE WEIGTHED DENSITY FUNCTIONAL THEORY

The term F_{att} represents the excess Helmholtz free-energy contribution due to the particle-particle attractive interaction, which can be described by the novel weighted density functional theory (WDFT) [S8] as the sum of a mean-field term and a correlation contribution, respectively, in the form

$$F_{\mathrm{att}}[\rho(\boldsymbol{r})] = \frac{1}{2}\int_V \mathrm{d}\boldsymbol{r}\int_V \mathrm{d}\boldsymbol{r}'\,\rho(\boldsymbol{r})u_{\mathrm{att}}(|\boldsymbol{r}-\boldsymbol{r}'|)\rho(\boldsymbol{r}') + k_BT\int_V \mathrm{d}\boldsymbol{r}\,\Phi_{\mathrm{corr}}(\bar{\rho}(\boldsymbol{r})), \tag{S17}$$

where the weighted density field is given by

$$\bar{\rho}(\boldsymbol{r}) = \int_V \mathrm{d}\boldsymbol{r}'\, \rho(\boldsymbol{r}')\bar{\omega}(\boldsymbol{r}-\boldsymbol{r}') \tag{S18}$$

where $\bar{\omega}(\boldsymbol{r}) = \Theta(d-|\boldsymbol{r}|)/(4\pi d^3/3)$, and $\Theta(x)$ is the Heaviside function. The Fourier transform of this weight function can be calculated using Eq. (S13) but changing $d/2$ to d. The correlation free-energy density is defined as

$$\Phi_{\mathrm{corr}}(\rho) = \beta\frac{F_{\mathrm{JZG}}(\rho)}{V} - \beta\frac{F_{\mathrm{hs}}(\rho)}{V} - \beta\rho^2 a_{\mathrm{mft}}, \tag{S19}$$

such that the excess Helmholtz free-energy of the bulk fluid coincides with the appropriated free-energy for the LJ fluid. The MFT parameter can be identified as the integral $a_{\mathrm{mft}} = 2\pi\int_0^\infty u_{\mathrm{att}}(r)r^2\,\mathrm{d}r = -(16/9)\pi\epsilon\sigma^3$.

The chemical potential is obtained by the bulk composition as

$$\mu^{\mathrm{att}} = \frac{\partial(F_{\mathrm{JZG}}(\rho_b)/V)}{\partial\rho^{(b)}}. \tag{S20}$$

IV. THE GRAND-POTENTIAL FUNCTIONAL DERIVATIVES

For a LJ fluid enclosed by a volume $\mathcal{V}$, with temperature T, and chemical potential μ specified, under the action of an external potential $\phi^{\mathrm{ext}}(\boldsymbol{r})$, the grand potential, Ω, is written as

$$\Omega[\rho(\boldsymbol{r})] = F^{\mathrm{id}}[\rho(\boldsymbol{r})] + F^{\mathrm{exc}}[\rho(\boldsymbol{r})] + \int_{\mathcal{V}}\mathrm{d}\boldsymbol{r}\,\big(\phi^{\mathrm{ext}}(\boldsymbol{r})-\mu\big)\rho(\boldsymbol{r}), \tag{S21}$$

where the ideal gas free-energy functional is written as

$$F^{\mathrm{id}}[\rho(\boldsymbol{r})] = k_BT\int_{\mathcal{V}}\mathrm{d}\boldsymbol{r}\,\rho(\boldsymbol{r})[\ln\big(\rho(\boldsymbol{r})\Lambda^3\big)-1], \tag{S22}$$

and the excess free energy functional is

$$F^{\mathrm{exc}}[\rho(\boldsymbol{r})] = F^{\mathrm{hs}}[\rho(\boldsymbol{r})] + F^{\mathrm{att}}[\rho(\boldsymbol{r})]. \tag{S23}$$

The variations are obtained keeping constant the chemical potentials μ, the external potential $\phi^{\mathrm{ext}}(\boldsymbol{r})$, the temperature T and the volume V.

$$\begin{aligned}\Omega[\rho+\delta\rho] = {} & F^{\mathrm{id}}[\rho+\delta\rho] + F^{\mathrm{hs}}[\rho+\delta\rho] + F^{\mathrm{att}}[\rho+\delta\rho] \\ & + \int_{\mathcal{V}}\mathrm{d}\boldsymbol{r}\,\big(\phi^{\mathrm{ext}}(\boldsymbol{r})-\mu\big)[\rho(\boldsymbol{r})+\delta\rho(\boldsymbol{r})],\end{aligned} \tag{S24}$$

where the variation of the ideal gas term is given by

$$\begin{aligned}
F^{\mathrm{id}}[\rho+\delta\rho] &= k_BT\int_{\mathcal{V}}\mathrm{d}\boldsymbol{r}\,[\rho(\boldsymbol{r})+\delta\rho(\boldsymbol{r})]\{\ln[(\rho(\boldsymbol{r})+\delta\rho(\boldsymbol{r}))\Lambda^3]-1\}\\
&= k_BT\int_{\mathcal{V}}\mathrm{d}\boldsymbol{r}\,[\rho(\boldsymbol{r})+\delta\rho(\boldsymbol{r})]\left\{\ln\big(\rho(\boldsymbol{r})\Lambda^3\big)+\frac{\delta\rho(\boldsymbol{r})}{\rho(\boldsymbol{r})}-1+\mathcal{O}(\delta\rho(\boldsymbol{r})^2)\right\}\\
&= k_BT\int_{\mathcal{V}}\mathrm{d}\boldsymbol{r}\,\{\rho(\boldsymbol{r})[\ln\big(\rho(\boldsymbol{r})\Lambda^3\big)-1]+\delta\rho(\boldsymbol{r})\ln\big(\rho(\boldsymbol{r})\Lambda^3\big)+\mathcal{O}(\delta\rho(\boldsymbol{r})^2)\},\\
&= F^{\mathrm{id}}[\rho]+k_BT\int_{\mathcal{V}}\mathrm{d}\boldsymbol{r}\,\{\delta\rho(\boldsymbol{r})\ln\big(\rho(\boldsymbol{r})\Lambda^3\big)+\mathcal{O}(\delta\rho(\boldsymbol{r})^2)\},
\end{aligned}\tag{S25}$$

the HS term is given by

$$F^{\mathrm{hs}}[\rho+\delta\rho]=F^{\mathrm{hs}}[\rho]+k_BT\sum_{\alpha}\iint_{\mathcal{V}}\mathrm{d}\boldsymbol{r}\,\mathrm{d}\boldsymbol{r}'\,\delta\rho(\boldsymbol{r})\frac{\partial n_\alpha(\boldsymbol{r}')}{\partial\rho(\boldsymbol{r})}\frac{\partial\Phi^{\mathrm{hs}}}{\partial n_\alpha(\boldsymbol{r}')}+\mathcal{O}(\delta\rho(\boldsymbol{r})^2),\tag{S26}$$

the WDFT term is given by

$$\begin{aligned}
F^{\mathrm{att}}[\rho+\delta\rho] &= F^{\mathrm{corr}}[\rho]+k_BT\iint_{\mathcal{V}}\mathrm{d}\boldsymbol{r}\,\mathrm{d}\boldsymbol{r}'\,\delta\rho(\boldsymbol{r})\frac{\partial\bar\rho(\boldsymbol{r}')}{\partial\rho(\boldsymbol{r})}\frac{\partial\Phi^{\mathrm{corr}}}{\partial\bar\rho(\boldsymbol{r}')}\\
&\quad\frac{1}{2}\iint_{\mathcal{V}}\mathrm{d}\boldsymbol{r}\,\mathrm{d}\boldsymbol{r}'\,[\rho(\boldsymbol{r})+\delta\rho(\boldsymbol{r})]u_{\mathrm{att}}(|\boldsymbol{r}-\boldsymbol{r}'|)[\rho(\boldsymbol{r}')+\delta\rho(\boldsymbol{r}')]\\
&= F^{\mathrm{corr}}[\rho]+\frac{1}{2}\iint_{\mathcal{V}}\mathrm{d}\boldsymbol{r}\,\mathrm{d}\boldsymbol{r}'\,\rho(\boldsymbol{r})u_{\mathrm{att}}(|\boldsymbol{r}-\boldsymbol{r}'|)\rho(\boldsymbol{r}')\\
&\quad k_BT\iint_{\mathcal{V}}\mathrm{d}\boldsymbol{r}\,\mathrm{d}\boldsymbol{r}'\,\delta\rho(\boldsymbol{r})\frac{\partial\bar\rho(\boldsymbol{r}')}{\partial\rho(\boldsymbol{r})}\frac{\partial\Phi^{\mathrm{corr}}}{\partial\bar\rho(\boldsymbol{r}')}+\iint_{\mathcal{V}}\mathrm{d}\boldsymbol{r}\,\mathrm{d}\boldsymbol{r}'\,\delta\rho(\boldsymbol{r})u_{\mathrm{att}}(|\boldsymbol{r}-\boldsymbol{r}'|)\rho(\boldsymbol{r}')+\mathcal{O}(\delta\rho(\boldsymbol{r})^2),
\end{aligned}\tag{S27}$$

and the weighted densities functional derivatives being

$$\frac{\partial n_\alpha(\boldsymbol{r}')}{\partial\rho(\boldsymbol{r})}=\int_{\mathcal{V}}\mathrm{d}\boldsymbol{r}''\,\delta(\boldsymbol{r}''-\boldsymbol{r})\omega^{(\alpha)}(\boldsymbol{r}'-\boldsymbol{r}'')=\omega^{(\alpha)}(\boldsymbol{r}'-\boldsymbol{r})\tag{S28}$$

$$\frac{\partial\bar\rho(\boldsymbol{r}')}{\partial\rho(\boldsymbol{r})}=\int_{\mathcal{V}}\mathrm{d}\boldsymbol{r}''\,\delta(\boldsymbol{r}''-\boldsymbol{r})\bar\omega(\boldsymbol{r}'-\boldsymbol{r}'')=\bar\omega(\boldsymbol{r}'-\boldsymbol{r})\tag{S29}$$

Therefore,

$$\begin{aligned}
\delta\Omega &= \Omega[\rho+\delta\rho]-\Omega[\rho]\\
&= k_BT\int_{\mathcal{V}}\mathrm{d}\boldsymbol{r}\,\delta\rho(\boldsymbol{r})\ln\big(\rho(\boldsymbol{r})\Lambda^3\big)+k_BT\sum_{\alpha}\iint_{\mathcal{V}}\mathrm{d}\boldsymbol{r}\,\mathrm{d}\boldsymbol{r}'\,\delta\rho(\boldsymbol{r})\omega^{(\alpha)}(\boldsymbol{r}'-\boldsymbol{r})\frac{\partial\Phi^{\mathrm{hs}}}{\partial n_\alpha(\boldsymbol{r}')}\\
&\quad+\iint_{\mathcal{V}}\mathrm{d}\boldsymbol{r}\,\mathrm{d}\boldsymbol{r}'\,\delta\rho(\boldsymbol{r})u_{\mathrm{att}}(|\boldsymbol{r}-\boldsymbol{r}'|)\rho(\boldsymbol{r}')\\
&\quad+k_BT\iint_{\mathcal{V}}\mathrm{d}\boldsymbol{r}\,\mathrm{d}\boldsymbol{r}'\,\delta\rho(\boldsymbol{r})\omega_{\mathrm{wdft}}(\boldsymbol{r}'-\boldsymbol{r})\frac{\partial\Phi^{\mathrm{corr}}}{\partial\bar\rho(\boldsymbol{r}')}+\int_{\mathcal{V}}\mathrm{d}\boldsymbol{r}\,\big(\phi^{\mathrm{ext}}(\boldsymbol{r})-\mu\big)\delta\rho(\boldsymbol{r}).
\end{aligned}\tag{S30}$$

Grouping the variational terms of $\delta\rho(\boldsymbol{r})$,we get

$$\begin{aligned}
\delta\Omega = \int_{\mathcal{V}}\mathrm{d}\boldsymbol{r}\,\delta\rho(\boldsymbol{r})\Bigg[&k_BT\ln\big(\rho(\boldsymbol{r})\Lambda^3\big)+k_BT\sum_{\alpha}\int_{\mathcal{V}}\mathrm{d}\boldsymbol{r}'\,\omega^{(\alpha)}(\boldsymbol{r}'-\boldsymbol{r})\frac{\partial\Phi^{\mathrm{hs}}}{\partial n_\alpha(\boldsymbol{r}')}\\
&+\int_{\mathcal{V}}\mathrm{d}\boldsymbol{r}'\,u_{\mathrm{att}}(|\boldsymbol{r}-\boldsymbol{r}'|)\rho(\boldsymbol{r}')+k_BT\int_{\mathcal{V}}\mathrm{d}\boldsymbol{r}'\,\omega_{\mathrm{wdft}}(\boldsymbol{r}'-\boldsymbol{r})\frac{\partial\Phi^{\mathrm{corr}}}{\partial\bar\rho(\boldsymbol{r}')}+\phi^{\mathrm{ext}}(\boldsymbol{r})-\mu\Bigg],
\end{aligned}\tag{S31}$$

Finally, the functional derivative is given as follows

$$\frac{\delta\Omega}{\delta\rho(\boldsymbol{r})} = k_BT\ln\big(\rho(\boldsymbol{r})\Lambda^3\big) - k_BTc^{(1)}(\boldsymbol{r}) + \phi^{\text{ext}}(\boldsymbol{r}) - \mu, \tag{S32}$$

where we define the 1st direct correlation function in the form

$$\begin{aligned} c^{(1)}(\boldsymbol{r}) = & -\sum_{\alpha}\int_{\mathcal{V}} \mathrm{d}\boldsymbol{r}'\,\omega^{(\alpha)}(\boldsymbol{r}'-\boldsymbol{r})\frac{\partial\Phi^{\text{hs}}}{\partial n_\alpha(\boldsymbol{r}')} - \beta\int_{\mathcal{V}}\mathrm{d}\boldsymbol{r}'\,u_{\text{att}}(|\boldsymbol{r}-\boldsymbol{r}'|)\rho(\boldsymbol{r}') \\ & -\int_{\mathcal{V}}\mathrm{d}\boldsymbol{r}'\,\omega_{\text{wdft}}(\boldsymbol{r}'-\boldsymbol{r})\frac{\partial\Phi^{\text{corr}}}{\partial\bar{\rho}(\boldsymbol{r}')} \end{aligned} \tag{S33}$$

Of course, the thermodynamic equilibrium condition is obtained by making

$$\left.\frac{\delta\Omega}{\delta\rho(\boldsymbol{r})}\right|_{\mu,V,T} = k_BT\ln\big(\rho(\boldsymbol{r})\Lambda^3\big) - k_BTc^{(1)}(\boldsymbol{r}) + \phi^{\text{ext}}(\boldsymbol{r}) - \mu = 0 \tag{S34}$$

where the equilibrium solution is a minimum with respect to the density profile.

The absolute adsorption quantity can be calculated by definition as

$$N_{\text{abs}} = \int_{V_{\text{uc}}}\rho(\boldsymbol{r})\,\mathrm{d}\boldsymbol{r}\,, \tag{S35}$$

where the local density distribution $\rho(\boldsymbol{r})$ is given by Eq. (S34).

V. EXCESS ADSORPTION ISOTHERMS

The excess adsorption quantity is calculated by

$$N_{\text{exc}} = N_{\text{abs}} - \rho_b V_{\text{pore}}, \tag{S36}$$

where V_{pore} is the pore volume. Experimentally, the pore volume can be obtained by He pycnometry [S9]. The V_{pore} can also be calculated by the 3D-cDFT as $V_{\text{pore}} = \int_{V_{\text{uc}}}\exp\Big[-\beta\phi^{(\text{He})}_{\text{ext}}(\boldsymbol{r})\Big]\,\mathrm{d}\boldsymbol{r}$, with the He LJ parameters $\sigma_{\text{He}} = 2.58$ Å, $\epsilon_{\text{He}}/k_B = 10.22$ K) [S10]. The Helium (He) void fraction, $V_{\text{pore}}/V_{\text{uc}}$, where V_{pore} is the pore volume obtained. For the aCarbon-Bhatia-id001 structure, the helium void fraction is computed to be 0.711, while for aCarbon-Marks-id002, it is 0.292. These values are in accordance with those documented in Ref. [S11], specifically 0.76 and 0.33, respectively. The reduced void fraction in aCarbon-Marks-id002 imposes a limitation on the adsorbed amount of CH_4 onto this structure.

VI. DENSITY ISOSURFACES

Here we present the density isosurfaces of CH_4 inside aCarbon-Bathia-id001 and aCarbon-Marks-id002 at 300 K and several pressure values with different orientations for visualization.

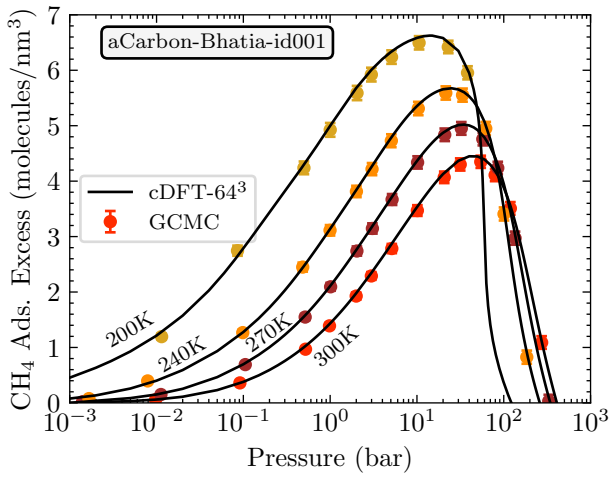

FIG. S2. Isotherms of the excess adsorption amount of CH_4 in aCarbon-Bhatia-id001 at temperature values of 200 K, 240 K, 270 K, and 300 K and a wide pressure range in logarithmic scale. Closed symbols: Our GCMC simulated data. Solid lines: Our cDFT results with $N^3 = 64^3$.

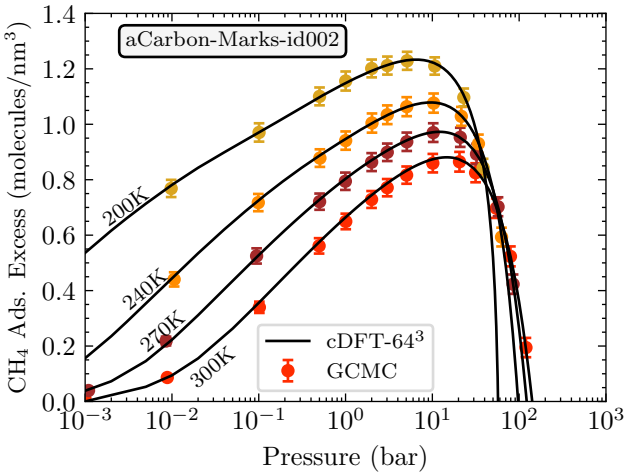

FIG. S3. Isotherms of the excess adsorption amount of CH_4 in aCarbon-Bhatia-id001 at temperature values of 200 K, 240 K, 270 K, and 300 K and a wide pressure range in logarithmic scale. Closed symbols: Our GCMC simulated data.Our cDFT results with $N^3 = 64^3$.

VII. COMPILED DATA OF GCMC AND CDFT

Here we present the simulated data from GCMC and calculated data from cDFT of CH_4 inside aCarbon-Bathia-id001 and aCarbon-Marks-id002 at several temperature and pressure values.

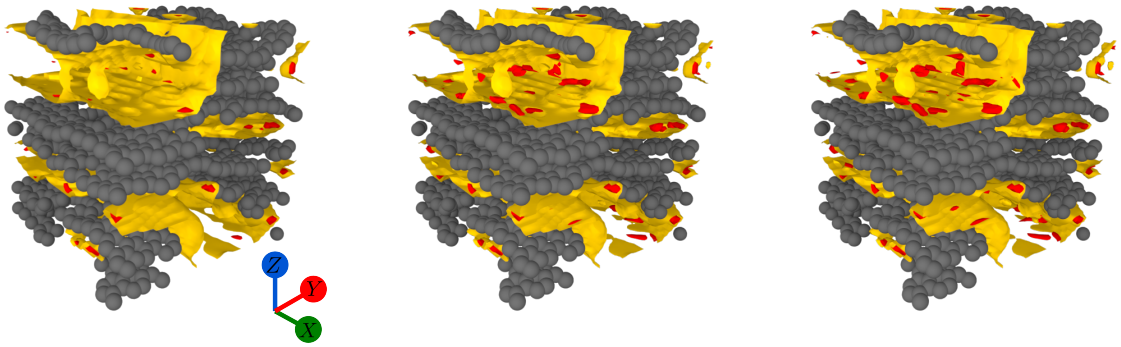

(a) 10 bar - 0 degrees (b) 100 bar - 0 degrees (c) 300 bar - 0 degrees

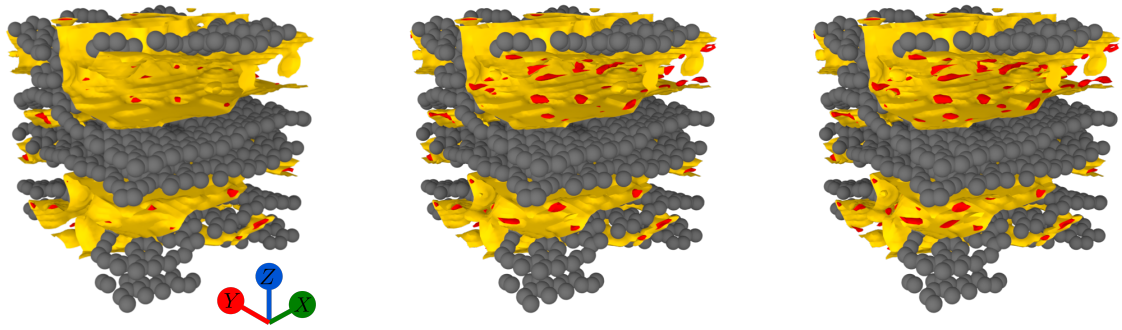

(d) 10 bar - 90 degrees (e) 100 bar - 90 degrees (f) 300 bar - 90 degrees

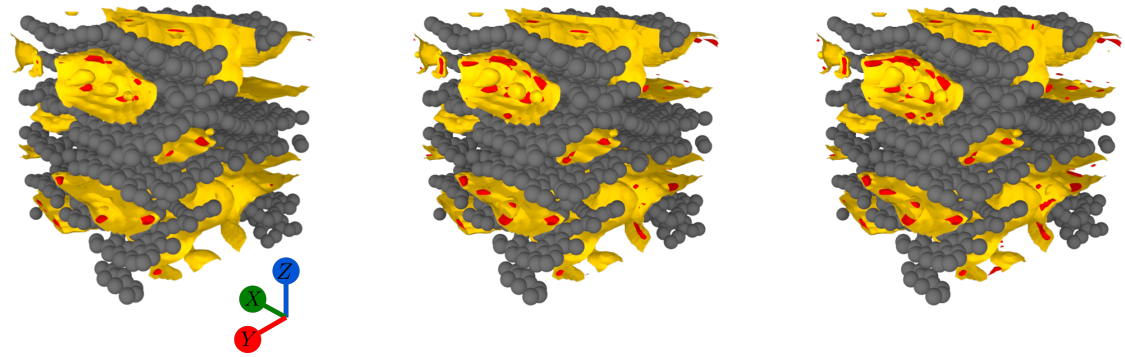

(g) 10 bar - 180 degrees (h) 100 bar - 180 degrees (i) 300 bar - 180 degrees

FIG. S4. Density isosurfaces of CH_4 in aCarbon-Bathia-id001 with local density values of 1 molecules/nm^3 (yellow) and 100 molecules/nm^3 (red) at the temperature of 300 K and three different pressures of (a,d,g) 10 bar, (b,e,h) 100 bar and (c,f,i) 300 bar. The different rows represent different angles around the z-axis.

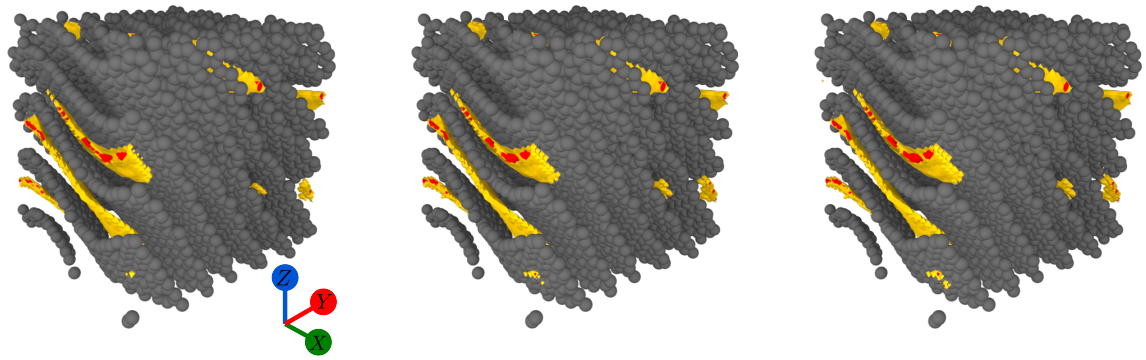

(a) 10 bar (b) 100 bar (c) 300 bar

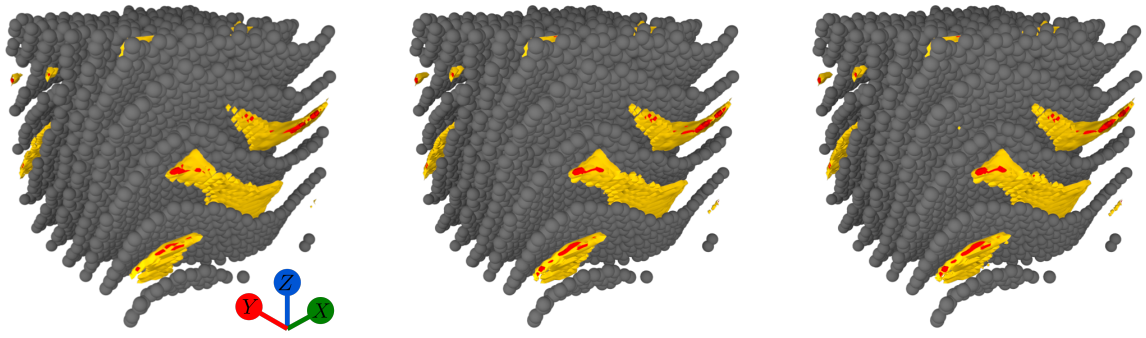

(d) 10 bar (e) 100 bar (f) 300 bar

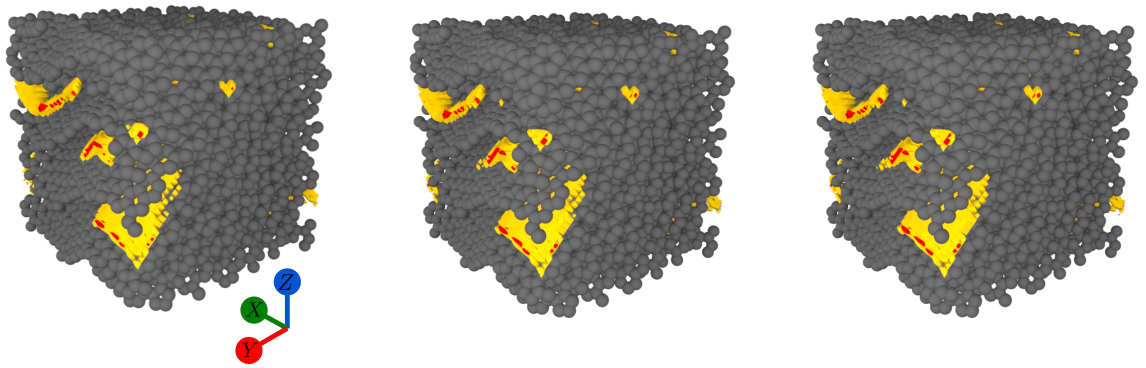

(g) 10 bar (h) 100 bar (i) 300 bar

FIG. S5. Density isosurfaces of CH_4 in aCarbon-Marks-id002 with local density values of 1 molecules/nm^3 (yellow) and 100 molecules/nm^3 (red) at the temperature of 300 K and three different pressures of (a,d,g) 10 bar, (b,e,h) 100 bar and (c,f,i) 300 bar. The different rows represent different angles around the z-axis.

TABLE S1. Absolute amount of CH_4 (in molecules/u.c.) adsorbed in aCarbon-Bathia-id001 at 300 K for wide pressure range (in bar).

P (bar)	**GCMC**	**DFT-32**[3]	**DFT-64**[3]
0.009	1.52(3)	1.55	1.36
0.102	9.61(2)	10.53	9.8
0.496	25.94(3)	27.13	25.97
1.006	37.36(5)	39.01	37.58
1.994	52.11(4)	53.88	52.13
3.017	62.15(1)	64.49	62.53
5.051	76.24(1)	79.03	76.74
10.124	96.75(5)	99.93	97.3
20.541	117.71(7)	121.09	118.38
31.484	129.18(5)	132.91	130.25
54.53	142.23(16)	146.11	143.54
79.35	149.95(7)	153.89	151.33
119.74	157.15(5)	161.17	158.61
195.554	164.6(3)	168.69	166.14
274.083	169.35(5)	173.64	171.08
RMSE	-	3.04	0.95

A. aCarbon-Bathia-id001

B. aCarbon-Marks-id002

[S1] M. G. Martin and J. I. Siepmann, Transferable potentials for phase equilibria. 1. United-atom description of n-alkanes, Journal of Physical Chemistry B **102**, 2569 (1998).

[S2] J. Gross and G. Sadowski, Perturbed-Chain SAFT: An Equation of State Based on a Perturbation Theory for Chain Molecules, Industrial & Engineering Chemistry Research **40**, 1244 (2001).

[S3] Y. Rosenfeld, Free-energy model for the inhomogeneous hard-sphere fluid mixture and density-functional theory of freezing, Physical Review Letters **63**, 980 (1989).

[S4] Y. X. Yu and J. Wu, Structures of hard-sphere fluids from a modified fundamental-measure theory, Journal of Chemical Physics **117**, 10156 (2002).

[S5] R. Roth, R. Evans, A. Lang, and G. Kahl, Fundamental measure theory for hard-sphere mixtures revisited: The white bear version, Journal of Physics Condensed Matter **14**, 12063 (2002).

TABLE S2. Absolute amount of CH_4 (in molecules/u.c.) adsorbed in aCarbon-Bathia-id001 at 270 K for wide pressure range (in bar).

P (bar)	**GCMC**	**DFT-32**[3]	**DFT-64**[3]
0.001	0.54(1)	0.11	0.1
0.009	4.01(1)	3.76	3.54
0.094	18.38(2)	18.15	17.86
0.502	41.33(2)	41.89	41.69
0.995	56.14(5)	56.62	56.35
1.997	73.84(5)	74.76	74.22
3.023	85.15(7)	86.54	85.79
5.072	99.99(4)	101.77	100.83
10.235	120.47(8)	122.64	121.66
20.964	139.58(5)	142.09	141.01
32.269	149.25(5)	152.03	150.8
57.134	159.61(12)	162.85	161.39
85.2	165.63(22)	169.05	167.47
136.146	171.74(36)	175.11	173.43
235.808	177.85(31)	181.44	179.7
329.733	181.98(46)	185.54	183.77
RMSE	-	2.30	1.23

[S6] Y. Rosenfeld, M. Schmidt, H. Löwen, and P. Tarazona, Fundamental-measure free-energy density functional for hard spheres: Dimensional crossover and freezing, Physical Review E **55**, 4245 (1997).

[S7] C. Kessler, J. Eller, J. Gross, and N. Hansen, Adsorption of light gases in covalent organic frameworks: comparison of classical density functional theory and grand canonical Monte Carlo simulations, Microporous and Mesoporous Materials **324**, 111263 (2021), arXiv:2103.12455.

[S8] Y.-X. Yu, A novel weighted density functional theory for adsorption, fluid-solid interfacial tension, and disjoining properties of simple liquid films on planar solid surfaces, The Journal of Chemical Physics **131**, 024704 (2009).

[S9] J. A. Myers, S. I. Sandler, and R. H. Wood, An Equation of State for Electrolyte Solutions Covering Wide Ranges of Temperature, Pressure, and Composition, Industrial & Engineering Chemistry Research **41**, 3282 (2002).

[S10] J. O. Hirschfelder, C. F. Curtiss, and R. B. Bird, *Molecular theory of gases and liquids* (John Wiley: New York, 1964).

[S11] R. Thyagarajan and D. S. Sholl, A database of porous rigid amorphous materials, Chemistry of Materials **32**, 8020 (2020).

TABLE S3. Absolute amount of CH_4 (in molecules/u.c.) adsorbed in aCarbon-Bathia-id001 at 240 K for wide pressure range (in bar).

P (bar)	**GCMC**	**DFT-32**[3]	**DFT-64**[3]
0.011	10.52(2)	11.22	10.96
0.099	33.66(2)	33.77	33.77
0.506	65.24(10)	66.24	66.2
1.003	83.19(10)	84.37	84
2.016	102.33(15)	103.89	103.31
3.025	113.73(12)	115.56	114.99
5.063	128.40(2)	130.52	129.99
10.335	146.79(21)	149.3	148.77
21.566	161.45(20)	164.67	163.62
33.953	168.67(33)	172.16	170.98
62.679	176.95(24)	180.31	178.87
101.197	181.52(28)	185.05	183.6
182.192	186.26(28)	189.81	188.35
315.628	191.18(6)	194.87	193.39
424.225	194.57(9)	198.2	196.7
RMSE	-	2.65	1.69

TABLE S4. Absolute amount of CH_4 (in molecules/u.c.) adsorbed in aCarbon-Bathia-id001 at 200 K for wide pressure range (in bar).

P (bar)	**GCMC**	**DFT-32**[3]	**DFT-64**[3]
0.01	31.72(3)	31.56	31.93
0.101	72.85(10)	73.69	74.25
0.501	113.12(15)	114.52	114.59
1.004	131.36(11)	133.32	133.44
2	150.00(15)	152.44	152.2
3.033	159.42(2)	162.47	161.86
5.119	169.37(18)	172.76	171.89
10.651	180.46(15)	183.78	182.91
23.02	189.4(2)	192.58	191.55
38.466	193.53(35)	197.22	196.27
127.368	199.3(2)	202.68	201.62
234.792	202.62(6)	205.95	204.78
298.455	204.6(4)	207.68	206.46
RMSE	-	2.77	2.10

TABLE S5. Absolute amount of CH_4 (in molecules/u.c.) adsorbed in aCarbon-Marks-id002 at 300 K for wide pressure range (in bar).

P (bar)	**GCMC**	**DFT-32**[3]	**DFT-64**[3]
0.009	4.71(1)	4.31	4.3
0.102	18.54(2)	20.05	18.91
0.496	30.75(4)	32.82	30.89
1.006	35.74(1)	38.14	36.03
1.994	40.44(13)	43.07	40.78
3.017	43.15(7)	45.96	43.55
5.051	46.41(2)	49.51	46.85
10.124	50.76(6)	54.19	51.13
20.541	55.22(13)	58.81	55.33
31.484	57.61(11)	61.47	57.81
54.53	60.73(9)	64.7	60.88
79.35	62.84(6)	66.77	62.89
119.74	64.89(19)	68.85	64.95
195.554	67.12(16)	71.15	67.28
274.083	68.86(8)	72.74	68.91
RMSE	-	3.21	0.27

TABLE S6. Absolute amount of CH_4 (in molecules/u.c.) adsorbed in aCarbon-Marks-id002 at 270 K for wide pressure range (in bar).

P (bar)	**GCMC**	**DFT-32**[3]	**DFT-64**[3]
0.001	2.15(1)	2.28	2.28
0.009	11.87(1)	11.28	10.91
0.094	28.62(8)	29.95	28.22
0.502	39.46(5)	41.91	39.86
0.995	43.68(8)	46.35	44.14
1.997	47.87(14)	50.79	48.23
3.023	50.24(6)	53.39	50.58
5.072	53.19(14)	56.61	53.46
10.235	57.27(6)	60.85	57.34
20.964	61.27(23)	64.87	61.19
32.269	63.45(21)	67.15	63.42
57.134	66.23(26)	69.93	66.19
85.2	67.88(8)	71.66	67.96
136.146	69.6(35)	73.46	69.82
235.808	71.69(11)	75.46	71.92
329.733	72.89(40)	76.82	73.35
RMSE	-	3.14	0.36

TABLE S7. Absolute amount of CH_4 (in molecules/u.c.) adsorbed in aCarbon-Marks-id002 at 240 K for wide pressure range (in bar).

P (bar)	**GCMC**	**DFT-32**[3]	**DFT-64**[3]
0.011	23.98(3)	26	24.51
0.099	39.11(9)	41.29	39.5
0.506	48.04(11)	50.92	48.58
1.003	51.72(6)	54.86	52.05
2.016	55.66(11)	58.84	55.62
3.025	57.78(3)	61.1	57.69
5.063	60.37(14)	63.87	60.31
10.335	63.74(17)	67.48	63.84
21.566	67.17(18)	70.83	67.28
33.953	69.11(3)	72.75	69.26
62.679	71.36(2)	75.04	71.64
101.197	72.89(22)	76.48	73.17
182.192	74.59(3)	78	74.8
315.628	76.08(15)	79.69	76.58
424.225	77.3(2)	80.86	77.8
RMSE	-	3.31	0.33

TABLE S8. Absolute amount of CH_4 (in molecules/u.c.) adsorbed in aCarbon-Marks-id002 at 200 K for wide pressure range (in bar).

P (bar)	**GCMC**	**DFT-32**[3]	**DFT-64**[3]
0.01	41.84(5)	43.8	42.39
0.101	52.89(20)	55.44	52.88
0.501	60.21(18)	63.39	60.06
1.004	63.52(35)	66.58	63.12
2	66.57(11)	69.55	66.09
3.033	67.75(24)	71.26	67.86
5.119	69.95(12)	73.32	70.05
10.651	72.44(17)	76.01	72.96
23.02	75.27(18)	78.45	75.66
38.466	76.56(55)	79.91	77.13
127.368	78.48(13)	81.71	78.96
234.792	79.46(15)	82.83	80.11
298.455	80.19(26)	83.45	80.74
RMSE	-	3.15	0.43